The intervening removable affinity tag (iRAT) production system facilitates Fv antibody fragment-mediated crystallography

AUTHOR(S):

Nomura, Yayoi; Sato, Yumi; Suno, Ryoji; Horita, Shoichiro; Iwata, So; Nomura, Norimichi

CITATION:

Nomura, Yayoi ...[et al]. The intervening removable affinity tag (iRAT) production system facilitates Fv antibody fragment-mediated crystallography. Protein Science 2016, 25(12): 2268-2276

ISSUE DATE:

2016-12

URL:

http://hdl.handle.net/2433/216542

The intervening removable affinity tag (iRAT) production system facilitates Fv antibody fragment-mediated crystallography

Yayoi Nomura[1,2], Yumi Sato[1,2], Ryoji Suno[1], Shoichiro Horita[1], So Iwata[1,2,3]*, and Norimichi Nomura[1,2]*

[1]Department of Cell Biology, Graduate School of Medicine, Kyoto University, Yoshida-Konoe-cho, Sakyo-ku, Kyoto 606-8501, Japan. [2]Japan Science and Technology Agency, Research Acceleration Program, Membrane Protein Crystallography Project, Yoshida-Konoe-cho, Sakyo-ku, Kyoto 606-8501, Japan. [3]RIKEN SPring-8 Center, Kouto, Sayo-cho, Sayo-gun, Hyogo 679-5148, Japan

Corresponding Authors:

So Iwata

Department of Cell Biology, Graduate School of Medicine, Kyoto University, Yoshida-Konoe-cho, Sakyo-ku, Kyoto 606-8501, Japan

Phone: 81-75-753-4372; Fax: 81-75-753-4660

E-mail: s.iwata@mfour.med.kyoto-u.ac.jp

Norimichi Nomura

Department of Cell Biology, Graduate School of Medicine, Kyoto University, Yoshida-Konoe-cho, Sakyo-ku, Kyoto 606-8501, Japan

Phone: 81-75-753-4389; Fax: 81-75-753-4660

E-mail: nnomura@mfour.med.kyoto-u.ac.jp

Running Title:

Fv antibody production via the iRAT system

Manuscript:

- Main-text: 27 pages
- Supplementary materials: 1 page

  Supplementary Figure 1 (Filename: iRAT_FigS1.tif)
- Three figures
- One table

Abstract:

Fv antibody fragments have been used as co-crystallization partners in structural biology, particularly in membrane protein crystallography. However, there are inherent technical issues associated with the large-scale production of soluble, functional Fv fragments through conventional methods in various expression systems. To circumvent these problems, we developed a new method, in which a single synthetic polyprotein consisting of a variable light (V_L) domain, an intervening removable affinity tag (iRAT), and a variable heavy (V_H) domain is expressed by a Gram-positive bacterial secretion system. This method ensures stoichiometric expression of V_L and V_H from the monocistronic construct followed by proper folding and assembly of the two variable domains. The iRAT segment can be removed by a site-specific protease during the purification process to yield tag-free Fv fragments suitable for crystallization trials. *In vitro* refolding step is not required to obtain correctly folded Fv fragments. As a proof of concept, we tested the iRAT-based production of multiple Fv fragments, including a crystallization chaperone for a mammalian membrane protein as well as FDA-approved therapeutic antibodies. The resulting Fv fragments were functionally active and crystallized in complex with the target proteins. The iRAT system is a reliable, rapid and broadly applicable means of producing milligram quantities of Fv fragments for structural and biochemical studies.

Keywords: antibody, Fv fragment, crystallization chaperone, membrane protein, therapeutic antibody, polyprotein, secretory expression, Gram-positive bacteria

A 50-75-word statement, written for a broader audience, outlining the importance and/or impact of the work presented in the manuscript:

Fv antibody fragments are versatile co-crystallization partners to aid the structural determination of otherwise 'uncrystallizable' proteins. In this study, we developed a fast and reliable method for production of Fv fragments in milligram quantities. The iRAT system is an accessible method for use in a broad range of antibody-mediated crystallography and structure-based research on the binding modes of therapeutic antibodies. Moreover, it may generally be applicable to the large-scale production of antibody reagents and therapeutics.

Introduction

Structural studies of key proteins that are involved in biologically and medically relevant molecular processes are frequently abandoned because of difficulties in preparing diffraction-quality crystals. In most cases, their molecular flexibility, conformational heterogeneity or polydispersal characteristics in solution hinders protein crystallization. Chaperone-assisted crystallography is a powerful strategy to address this problem and can be applied to a broad range of membrane proteins and otherwise 'uncrystallizable' soluble proteins, such as heavily glycosylated and multi-domain proteins[1,2]. The chaperone molecules aid in crystallization by increasing the hydrophilic surface area available for rigid crystal lattice formation. The bound chaperone molecules reduce the inherent protein flexibility and conformational heterogeneity, thereby increasing the chance of successful crystallization of difficult target proteins.

Different protein scaffolds have been used as crystallization chaperones, ranging from animal-derived antibody fragments[3,4] to synthetic binders such as DARPins[5] and Monobodies[6]. DNA and RNA aptamers have also been applied as co-crystallization partners[7,8]. Among the reported chaperones, Fv antibody fragment is a promising scaffold that has been used to crystallize of a variety of membrane proteins including bacterial cytochrome *c* oxidase[9,10], yeast cytochrome bc_1 complex[11], archaeal KvAP voltage-gated potassium channel[12], human adiponectin receptors[13] and the mammalian fructose transporter GLUT5[14]. In addition, the compactness of Fv fragments affords additional advantages in structural studies examining the antigen-antibody interface, such as the characterization of therapeutic antibody blocking mechanisms[15,16].

Preparation of milligram quantities of purified Fv fragments is the most critical prerequisite when Fv fragments are used as co-crystallization partners. Several studies evaluating the quantity and quality of Fv fragments produced from different expression systems have been performed. Bicistronic V_L-V_H overexpression in the *Escherichia coli* periplasm results in relatively low yields (0.5-1 mg per liter of culture)[17]. Recovery of functional Fv fragments from *E. coli* cytoplasmic inclusion bodies requires a laborious and time-consuming refolding process during purification[18]. In contrast, Gram-positive bacteria lack an outer membrane and have a powerful secretion apparatus that allows disulfide bond formation and the proper folding of antibody fragments in an oxidizing environment. Bicistronic V_L-V_H secretory expression has been tested in *Streptomyces lividans* to purify a certain Fv fragment[19], but it is not known whether this method can be practically applied to a wide range of antibody clones. Production of Fv fragments by two-membered culture of the separate V_L- and V_H-expression strains in *Brevibacillus chosinensis* secretory system[14] is problematic when either strain proliferates too rapidly.

To solve these problems, we have developed a new expression strategy in which the stoichiometric secretion and assembly of the V_L and V_H domains are achieved by monocistronic expression in the Gram-positive bacterium *B. choshinensis*. A polyhistidine-maltose binding protein (His_6-MBP) cassette, embedded within the intervening region of the two variable domains, serves as an affinity purification tag that can be removed by tobacco etch virus (TEV) protease cleavage. We chose the name “iRAT (intervening removable affinity tag) system” to describe this production strategy. Here, we present a reliable and

broadly applicable method for preparing milligram quantities of Fv fragments. This method was validated through the production of multiple Fv fragments derived from murine and humanized monoclonal antibodies including therapeutic antibodies approved by the U.S. Food and Drug Administration (FDA). The suitability of the resulting Fv fragments for structural studies was also demonstrated through co-crystallization and X-ray diffraction analyses.

Results

Concept and development of the iRAT system

We developed the iRAT system to address the need for a reliable method to control the 1:1 stoichiometric expression and the proper folding of the V_L and V_H domains, each of which contains an intrachain disulfide bond. To increase the throughput of crystallization trials, it is ideal to collect soluble and functional Fv fragments with high yields by using simple purification procedures without *in vitro* refolding, a time and labor intensive process. Considering these prerequisites, we generated a synthetic polyprotein encoding both the V_L and V_H domains by using a monocistronic expression strategy in a Gram-positive bacterial secretion system. Specifically, the new expression vector pBIM2 contained the V_L- and V_H-coding sequences cloned in a single reading frame (Fig. 1A). The two variable domains were tethered together by the iRAT segment, which contained the first TEV cleavage site, the His_6 tag, a linker, MBP, another linker and the second TEV cleavage site in that order. The iRAT portion can be removed by cleavage with His_6-tagged TEV protease (TEV-His_6) followed by

reverse immobilized metal-affinity chromatography (IMAC) (Fig. 1B and Methods). MBP was included to enhance the secretory expression of the synthetic polyprotein. The purification yields for iRAT-based Fv expression were 1.5 to 1.7-fold higher than those of the non-MBP fusion. Another reason for including MBP is that the distance between the N- and C-termini (43 Å) is similar to the distance between the C-terminus of V_L and the N-terminus of V_H (approximately 35-40 Å) for most Fv fragments[20]. The construct was cloned downstream of the constitutively active promoter P5 and the Sec signal peptide for polyprotein secretion into the culture supernatant.

iRAT-based production of a crystallization chaperone for the rat fructose transporter GLUT5

In a previous study, an Fv fragment (clone number: 4D111) was used to improve the crystallization of the rat GLUT5 fructose transporter[14]. We tested the large-scale expression and purification of the Fv 4D111 by using the iRAT system. *Brevibacillus* cells harboring the pBIM2-based construct were cultivated for 48 h. Afterward, Fv 4D111 was purified from the culture supernatant by using ammonium sulfate precipitation followed by IMAC, TEV cleavage, reverse IMAC and size exclusion chromatography (SEC) (Methods). The yield of purified Fv 4D111 was 4.1 mg per liter of culture, and no apparent aggregation occurred when the purified protein was concentrated to ~10 mg/mL. A typical SEC elution profile for Fv 4D111 is shown in Figure 2A. The elution peak was monodisperse, and oligomer formation was not observed. Calibration with molecular standards revealed that the Fv 4D111 existed as a monomer in solution with an apparent

molecular weight of ~26 kDa. SDS-PAGE under reducing conditions showed a double band with the expected mobility of the V_L and V_H domains (Fig. 2B).

To test whether the purified Fv fragment was functional, SEC of the rat GLUT5 transporter in complex with Fv 4D111 was performed. A molar excess of Fv 4D111 was mixed with GLUT5 and loaded onto an SEC column. Complex formation was indicated by an elution peak shift toward higher molecular weights, as compared with uncomplexed GLUT5 (Fig. 2C). SDS-PAGE analysis of the high molecular weight peak clearly showed the presence of both GLUT5 and Fv 4D111 (Fig. 2D). Surface plasmon resonance (SPR) experiments indicated that iRAT-produced Fv 4D111 bound GLUT5 with a K_D value of 2.4 nM (Fig. 2E). The thermal stability of GLUT5 in the presence or absence of Fv 4D111 indicated that this antibody fragment increased the *T*m by 12.5°C after GLUT5 binding, thus suggesting that Fv 4D111-bound GLUT5 was significantly stabilized (Fig. 2F). Furthermore, the GLUT5-Fv 4D111 complex was able to be crystallized (Fig. 2G, inset). The co-crystals diffracted up to 3.2 Å and generated complete diffraction sets, which were able to be processed to solve the structure of the GLUT5-Fv complex (Fig. 2G). These results suggest that the iRAT system is useful for the production of Fv scaffold-based crystallization chaperones in milligram quantities.

iRAT-based production of Fv fragments of therapeutic antibodies for co-crystallization with their targets

A structure-based understanding of the interactions between therapeutic

antibodies and target proteins is critical to the rational design of improved biotherapeutics. However, a relatively small number of crystal structures have been determined for therapeutic antibody-target protein complexes, which probably reflects the lack of simple methods facilitating production of recombinant antibody fragments in milligram quantities, resulting in limited success in co-crystallization trials. Typical examples include certolizumab and denosumab. Certolizumab is a humanized monoclonal antibody that targets the tumor necrosis factor α (TNFα) and is used to treat rheumatoid arthritis and Crohn's disease[21]. Denosumab is a human monoclonal antibody that targets the receptor activator of nuclear factor κB ligand (RANKL) and is used to treat osteoporosis, treatment-induced bone loss, metastases to bone, and giant cell tumors of the bone[22]. Although the U.S. FDA has approved these two antibodies, the interactions between the antibodies and their target molecules have not been accurately mapped at atomic-level resolution by crystallographic analyses. To demonstrate the utility of the iRAT system, we produced Fv fragments derived from these two therapeutic antibodies.

Amino acid sequence data for the antibodies were retrieved from DrugBank (http://www.drugbank.ca/). Codon-optimized cDNAs encoding the V_L and V_H domains were artificially synthesized and cloned into the pBIM2 vector. The certolizumab Fv and the denosumab Fv were readily expressed and purified to greater than 95% purity with yields of 15.4 and 1.0 mg per liter of culture, respectively. Excess amounts of each of the purified Fv fragments were mixed with the corresponding target protein. The resulting complexes appeared to be monodisperse, as indicated by the SEC analysis (Figs. 3A and 3D). SDS-PAGE

analysis confirmed that the higher-molecular-weight peak fractions contained the Fv fragment and its target cytokine, thus indicating tight complex formation between them (Figs. 3B and 3E). Purified, concentrated complexes were used to set up broad crystallization screens, and the crystallization conditions were then optimized by varying the precipitant concentration. Promising crystals whose complete diffraction data sets were collected are shown in Figures 3C and 3F. The data collection statistics are shown in Table 1. Molecular replacement was performed using the Fv 4D111 structure (PDB ID: 4YBQ, chains C and D) as the search model, and interpretable electron-density maps were obtained. Electron densities corresponding to either TNFα or RANKL were observed, and model building and structure refinement are under way.

Discussion

Fab fragments are the most commonly used crystallization chaperones. However, they are relatively large co-crystallization partners of approximately 500 amino acids, and they often generate crystal lattices with one or more large cell edges, which can cause diffraction spots to overlap and complicate structural determination. The flexibility of the elbow angle between the variable and constant domains in Fab fragments sometimes hinders crystallization. Fv fragments can be used as complementary and alternative crystallization chaperones with having all the features of the binding interface present in larger Fab fragments. Single-chain Fv (scFv) fragments are similar to Fv fragments, but the linker between the V_L and V_H domains makes scFv fragments prone to forming intermolecularly domain-swapped dimers[23]. The dimer-monomer

equilibrium of scFv fragments can increase structural heterogeneity; therefore, an antibody in scFv format is less desirable for crystallization. In addition, Fv fragments are less prone to distortion than scFv fragments because aggregation of scFv fragments is sensitive to the linker length. Nanobodies (VHHs) are increasingly finding favor with crystallographers due to their small size, ease of expression and purification, and extreme structural stability. Another fascinating feature of Nanobodies is their extended convex paratope structure that can bind deep into molecular clefts to trap the target in a particular conformational state[4]. However, Fv fragments have an advantage over Nanobodies in more efficient enlargement of hydrophilic surfaces for crystal contacts because of the larger molecular size.

Fv fragments are heterodimeric molecules consisting of two domains, V_L and V_H, that assemble through hydrophobic interactions. Each of the V_L and V_H domains contains an intrachain disulfide bond for stabilization. These structural properties require a sophisticated apparatus for secretion, folding, and assembly as well as an oxidizing environment for disulfide bond generation. *B. choshinensis* is well known for its capacity to secrete large amounts of proteins directly into the culture medium. Expression of Fv fragments via the *B. choshinensis* Sec-dependent secretion pathway ensures the formation of the intrachain disulfide bonds to stabilize the structure. Thus, we combined the advantages of monocistronic stoichiometric expression with those of Gram-positive bacterial secretory expression to develop the iRAT system. To make this system suitable for structural studies, the linker segment that tethers the V_L and V_H domains can be cleaved by the site-specific protease and removed during the purification

process.

The iRAT system is a streamlined pipeline that provides the desired intermediate throughput to produce many Fv fragments in parallel. The typical duration for running one cycle of the iRAT-production procedure, from plasmid construction to protein purification, is 10 days. The procedure is easy and cost-effective and does not require any time-consuming or labor-intensive steps. The iRAT system generally produces high Fv fragment purification yields sufficient for structural studies. We have tested the iRAT-based expression and purification of randomly chosen 17 different Fv fragments and found that the yields exceed 3 mg per liter of culture in 12 out of them (data not shown). These yields considerably exceed those obtained from equivalent constructs expressed in the *E. coli* periplasm. A limitation of the iRAT system is the yield variability among individual antibody clones, which can be attributed to the sequence of the variable domains and the stability of the hydrophobic interactions between them. However, we have not identified specific sequence motifs and other factors that affect the yields; hence the yield cannot be judged in advance on the basis of the sequence information alone.

Overall, the iRAT production system is an accessible method for use in a broad range of Fv antibody-mediated crystallography and structure-based research on the binding modes of therapeutic antibodies. Moreover, it may generally be applicable to the large-scale production of antibody reagents and therapeutics.

Methods

Plasmid construction

The pBIM2 vector (Fig. 1A) for expression of Fv fragments was designed on the basis of the backbone of the *Brevibacillus* plasmid pNY326 (Clontech). The V_L-insertion site, iRAT cassette and V_H-insertion site were tandemly arranged in this order and introduced downstream of the constitutively active P5 promoter and the Sec secretion signal sequence. The iRAT cassette encoded the N-terminal TEV cleavage site, His_6 tag, a 9-residue Gly/Ser-rich linker, the MBP coding sequence (residues 27 to 392 from UniProt ID: P0AEX9), a 25-residue Asn/Gly/Ser-rich linker and a C-terminal TEV cleavage site (Supplementary Fig. 1). Residues 1-107 (Kabat numbering scheme) of the V_L domain and 1-113 of the V_H domain derived from monoclonal antibodies were used for Fv fragment expression. The artificially synthesized, codon-optimized cDNAs encoding the V_L and V_H domains were amplified with primers that included 5' overhangs (27 bp) complementing the upstream and downstream sequences to the pBIM2 vector junctions. The iRAT segment was amplified with the two primers BIM2-F (5'-ACTAGTGAAAATTTATATTTTCAAGGTCACCATCACCATCACCATTCCTCTGGTGGC GGT) and BIM2-R (5'-AAGCTTCGATTGGAAGTACAGGTTTTCGGAAGATCTAGAGGAACCACCCCCACCCCC GAG). The pNY326 backbone was amplified with the two primers pNY326-F (5'-GAATTCGGTACCCCGGGTTCGA) and pNY326-R (5'-GGATCCTGCAGCGAAAGCCATGGGAGC). A total of four PCR-amplified DNA fragments for each antibody clone were added to Gibson Assembly Master Mix (New England Biolabs) and incubated at 50°C for 60 min. *B. choshinensis* HPD31-

SP3 cells (Clontech) were electroporated with the assembled DNA under conditions of 7.5 kV/cm, 25 μF, and 1000 Ω. The transformants were selected on plates supplemented with 50 mg/L neomycin. The resulting plasmids were extracted with a conventional miniprep kit. For SPR experiments, a derivative of Fv 4D111 with an HA tag at the C-terminus of the V_H domain was constructed. Preparation of the pBIM2-based plasmid typically took 3 days.

Construction of the expression plasmid for *Homo sapiens* TNFα was also on the basis of the pNY326 plasmid backbone. The extracellular domain of human TNFα (UniProt ID: P01375, residues 77 to 233) was FLAG-tagged at the N-terminus. To facilitate detection and purification, a TEV cleavage site and His_6-HA tag were added at the C-terminus. The construct was inserted downstream of the P5 promoter and Sec secretion signal sequence.

Construction of the expression plasmid for *H. sapiens* RANKL was based on the backbone of the *E. coli* plasmid pBAD-*Myc* His (Thermo Fisher Scientific). The extracellular domain of human RANKL (UniProt ID: O14788, residues 162 to 317) was fused with NusA, a His_6 tag, a 23-residue linker and a TEV cleavage site at the N-terminus. The construct was inserted downstream of the P_{BAD} promoter. *E. coli* TOP10 cells (Thermo Fisher Scientific) were transformed with the resulting plasmid. The transformants were selected on LB plates supplemented with 100 mg/L ampicillin. All of the cloned inserts were verified by sequencing both strands.

Protein expression and purification

The Fv fragments and human TNFα were expressed in *B. choshinensis* and secreted into the culture medium. *B. choshinensis* cells harboring the expression plasmids were grown overnight at 30°C and 200 rpm in 2SY medium (soytone 40 g/L, yeast extract 5 g/L, glucose 20 g/L, and $CaCl_2$ 0.15 g/L) supplemented with 50 mg/L neomycin. The culture was diluted 1:100 into 1 L of 2SY medium in 2.5 L baffled Tunair shaker flasks and grown for 48-60 h. The cells were removed by centrifugation at 6,000 *g* for 15 min. The culture supernatant was adjusted to a final ammonium sulfate concentration of 60% saturation. The precipitate was pelleted, dissolved in TBS buffer (10 mM Tris-HCl, pH 7.5, 150 mM NaCl), and dialyzed overnight against the same buffer. The dialyzed sample was mixed with Ni-NTA resin (Qiagen) equilibrated with buffer A (10 mM Tris-HCl, pH 7.5, 150 mM NaCl, and 20 mM imidazole). Bound proteins were eluted with buffer B (10 mM Tris-HCl, pH 7.5, 150 mM NaCl, and 250 mM imidazole), mixed with TEV-His_6 and dialyzed overnight against TBS buffer. The cleaved His_6-tagged portion (the iRAT segment of the Fv-containing polyprotein or C-terminal His_6-HA tag of the TNFα) and TEV-His_6 were removed using a HisTrap HP column (GE Healthcare) equilibrated with buffer A. The flow-through fractions were concentrated and loaded onto a HiLoad16/60 Superdex75 column (GE Healthcare) equilibrated with TBS buffer. The peak fractions were pooled, concentrated, flash frozen in liquid nitrogen, and stored at -80°C. The typical duration for this procedure was 7 days.

E. coli TOP10 cells harboring the expression plasmid for human RANKL were grown overnight at 37°C and 250 rpm in LB supplemented with 100 mg/L ampicillin. The culture was diluted 1:100 into 200 mL of the same medium and

grown at 37°C to an OD_{600} of 0.5 followed by overnight incubation at 20°C with 0.02% arabinose. The cells were harvested by centrifugation at 6,000 *g* for 15 min and re-suspended in buffer S1 (10 mM Tris-HCl, pH 8.0, 150 mM NaCl, 20 mM imidazole, 0.1% Triton X-100, Roche EDTA-free protease inhibitor tablet). Cells were disrupted by sonication followed by DNaseI treatment on ice for 30 min. The lysate was clarified via centrifugation and loaded onto a HisTrap Crude column (GE Healthcare) equilibrated with buffer A. Bound proteins were eluted with buffer B, mixed with TEV-His_6 and dialyzed overnight against TBS buffer. The cleaved NusA-His_6 tag and TEV-His_6 were removed using a HisTrap HP column equilibrated with buffer A. The flow-through fractions were concentrated and loaded onto a Superdex200 10/300GL column (GE Healthcare) equilibrated with TBS buffer. The peak fractions were pooled, concentrated, flash frozen in liquid nitrogen, and stored at -80°C.

Rat GLUT5 was expressed and purified using previously described methods[14].

SPR experiments

SPR experiments were performed at 20°C using a Biacore T100 with series S streptavidin sensor chips (Series S sensor chip SA; GE Healthcare) in TBS containing 0.05% dodecyl-β-D-maltopyranoside (DDM). Biotinylated anti-HA IgG (Rockland Immunochemicals) was captured on the streptavidin surface (flow cells 1 and 2) with a 400 sec injection of 50 µg/mL of antibody at 10 µL/min. Purified samples of the HA-tagged Fv 4D111 with 12 mg/mL BSA and 12 mg/mL

CM-dextran were subsequently injected (500 µL at a flow rate of 10 µL/min) over flow cell 2. GLUT5 at various concentrations was simultaneously passed over flow cells 1 and 2 at a flow rate of 30 µL/min. Association and dissociation times were 2 and 5 min, respectively. Regeneration consisted of a 30 sec injection of 10 mM NaOH. Flow cell 1 was used as a reference surface. Data analysis was performed using BIAevaluation software (GE Healthcare).

Thermal stability assay

The thermal stability of GLUT5 was evaluated in the presence or absence of Fv 4D111 using the thiol-specific fluorochrome N-[4-(7-diethylamino-4-methyl-3-coumarinyl)phenyl]maleimide (CPM), as described previously[24] with minor modifications. Briefly, 19.5 µL GLUT5 or GLUT5-Fv 4D111 complex (0.2 nmol) in TBS containing 0.02% DDM was mixed with 0.5 µL CPM dye (4 mg/mL). The reaction mixture was transferred to a clean PCR tube and heated with a ramp rate of 3°C/min in a My iQ2 thermal cycler (Bio-Rad). The excitation wavelength was set to 365 nm and the emission wavelength was set to 460 nm. Assays were performed over a temperature range of 4°C to 80°C. Melting temperatures (*T*m) were determined by fitting the curves to a sigmoidal dose-response equation.

Crystallization

The protein complex was prepared by incubating the target protein with the Fv fragment at a molar ratio of 1:2 for 1 h on ice. Size exclusion chromatography was performed on the complex (Superdex 200 10/300 column, GE Healthcare),

which was equilibrated with TBS containing 0.02% DDM (GLUT5-Fv 4D111) or TBS (TNFα-certolizumab Fv and RANKL-denosumab Fv). Peak fractions containing the complexes were concentrated to approximately 10 mg/mL by ultrafiltration (Millipore, MWCO 10 kDa) and used for the crystallization experiments.

The crystals used for the X-ray diffraction experiments were grown for 14-20 days at 20°C by hanging drop vapor diffusion. A 400 μL reservoir was equilibrated against a 2 μL drop containing a 1:1 mixture of the complex and reservoir solution. For GLUT5-Fv 4D111 co-crystallization, the reservoir contained 0.1 M Tris-HCl (pH 8.0), 0.12 M $CaCl_2$ and 33-35% PEG400. For TNFα-certolizumab Fv co-crystallization, the reservoir contained 0.1 M tri-sodium citrate/citric acid (pH 5.6) and 50% PEG3000. For RANKL-denosumab Fv co-crystallization, the reservoir contained 0.1 M sodium acetate/acetic acid (pH 4.6) and 2 M NaCl. The GLUT5-Fv 4D111 co-crystals were flash-frozen in liquid nitrogen. The co-crystals of TNFα-certolizumab Fv and RANKL-denosumab Fv were cryo-protected in 25% ethylene glycol in the mother liquor and then flash-frozen in liquid nitrogen.

Diffraction data collection and analysis

The diffraction data were collected at 100 K at the SPring-8 beamline BL41XU (Japan) using a MX225HE (Rayonix) or PILATUS3 6M (Dectris) detector. The data were then integrated and scaled using HKL2000[25] or XDS[26]. Molecular replacement was performed with the MR-PHASER program[27]. The atomic

coordinates of Fv 4D111 (PDB ID: 4YBQ, chains C and D) served as the search models. The model was further rebuilt in COOT[28].

Acknowledgments

The diffraction data were collected at SPring-8 (Proposal Nos. 2015A1104 and 2016A2570) with the excellent assistance of the beamline scientists. This work was funded by the Research Acceleration Program of the Japan Science and Technology Agency (JST); by the Platform for Drug Discovery, Informatics, and Structural Life Science of the Ministry of Education, Culture, Sports, Science and Technology (MEXT) of Japan; and by Grants-in-Aids for Scientific Research from the Japan Society for the Promotion of Science (JSPS) (Nos. 15K06968 and 15J04343). S. H. is a recipient of a JSPS postdoctoral fellowship.

Supplementary Material Filenames

Supplementary Figure 1 (Filename: iRAT_FigS1.tif)

Conflicts of Interest Statement

The authors declare no conflict of interest associated with this manuscript.

References

1. Griffin L, Lawson A (2011) Antibody fragments as tools in crystallography. Clin Exp Immunol 165:285-291.

2. Lieberman RL, Culver JA, Entzminger KC, Pai JC, Maynard JA (2011) Crystallization chaperone strategies for membrane proteins. Methods 55:293-302.

3. Hino T, Iwata S, Murata T (2013) Generation of functional antibodies for mammalian membrane protein crystallography. Curr Opin Struct Biol 23:563-568.

4. Pardon E, Laeremans T, Triest S, Rasmussen SG, Wohlkönig A, Ruf A, Muyldermans S, Hol WG, Kobilka BK, Steyaert J (2014) A general protocol for the generation of Nanobodies for structural biology. Nat Protoc 9:674-693.

5. Sennhauser G, Grütter MG (2008) Chaperone-assisted crystallography with DARPins. Structure 16:1443-1453.

6. Lu M, Symersky J, Radchenko M, Koide A, Guo Y, Nie R, Koide S (2013) Structures of a Na^+-coupled, substrate-bound MATE multidrug transporter. Proc Natl Acad Sci USA 110:2099-2104.

7. Kato K, Ikeda H, Miyakawa S, Futakawa S, Nonaka Y, Fujiwara M, Okudaira S, Kano K, Aoki J, Morita J, Ishitani R, Nishimasu H, Nakamura Y, Nureki O (2016) Structural basis for specific inhibition of Autotaxin by a DNA aptamer. Nat Struct Mol Biol 23:395-401.

8. Nomura Y, Sugiyama S, Sakamoto T, Miyakawa S, Adachi H, Takano K, Murakami S, Inoue T, Mori Y, Nakamura Y, Matsumura H (2010) Conformational plasticity of RNA for target recognition as revealed by the 2.15 Å crystal structure of a human IgG-aptamer complex. Nucleic Acids Res 38:7822-7829.

9. Iwata S, Ostermeier C, Ludwig B, Michel H (1995) Structure at 2.8 Å resolution of cytochrome *c* oxidase from *Paracoccus denitrificans*. Nature 376:660-669.

10. Ostermeier C, Iwata S, Ludwig B, Michel H (1995) Fv fragment-mediated crystallization of the membrane protein bacterial cytochrome *c* oxidase. Nat Struct Biol 2:842-846.

11. Hunte C, Koepke J, Lange C, Rossmanith T, Michel H (2000) Structure at 2.3 Å resolution of the cytochrome bc_1 complex from the yeast *Saccharomyces cerevisiae* co-crystallized with an antibody Fv fragment. Structure 8:669-684.

12. Lee SY, Lee A, Chen J, MacKinnon R (2005) Structure of the KvAP voltage-dependent K^+ channel and its dependence on the lipid membrane. Proc Natl Acad Sci USA 102:15441-15446.

13. Tanabe H, Fujii Y, Okada-Iwabu M, Iwabu M, Nakamura Y, Hosaka T, Motoyama K, Ikeda M, Wakiyama M, Terada T, Ohsawa N, Hato M, Ogasawara S, Hino T, Murata T, Iwata S, Hirata K, Kawano Y, Yamamoto M, Kimura-Someya T, Shirouzu M, Yamauchi T, Kadowaki T, Yokoyama S (2015) Crystal structures of the human adiponectin receptors. Nature 520:312-316.

14. Nomura N, Verdon G, Kang HJ, Shimamura T, Nomura Y, Sonoda Y, Hussien SA, Qureshi AA, Coincon M, Sato Y, Abe H, Nakada-Nakura Y, Hino T, Arakawa

T, Kusano-Arai O, Iwanari H, Murata T, Kobayashi T, Hamakubo T, Kasahara M, Iwata S, Drew D (2015) Structure and mechanism of the mammalian fructose transporter GLUT5. Nature 526:397-401.

15. Hwang WC, Lin Y, Santelli E, Sui J, Jaroszewski L, Stec B, Farzan M, Marasco WA, Liddington RC (2006) Structural basis of neutralization by a human anti-severe acute respiratory syndrome spike protein antibody, 80R. J Biol Chem 281:34610-34616.

16. Sui J, Hwang WC, Perez S, Wei G, Aird D, Chen LM, Santelli E, Stec B, Cadwell G, Ali M, Wan H, Murakami A, Yammanuru A, Han T, Cox NJ, Bankston LA, Donis RO, Liddington RC, Marasco WA (2009) Structural and functional bases for broad-spectrum neutralization of avian and human influenza A viruses. Nat Struct Mol Biol 16:265-273.

17. Mir SH, Escher C, Kao WC, Birth D, Wirth C, Hunte C (2015) Generation of recombinant antibody fragments for membrane protein crystallization. Methods Enzymol 557:201-218.

18. Tsumoto K, Shinoki K, Kondo H, Uchikawa M, Juji T, Kumagai I (1998) Highly efficient recovery of functional single-chain Fv fragments from inclusion bodies overexpressed in *Escherichia coli* by controlled introduction of oxidizing reagent - application to a human single-chain Fv fragment. J Immunol Methods 219:119-129.

19. Ueda Y, Tsumoto K, Watanabe K, Kumagai I (1993) Synthesis and expression of a DNA encoding the Fv domain of an anti-lysozyme monoclonal antibody, HyHEL10, in *Streptomyces lividans*. Gene 129:129-134.

20. Gilmartin AA, Lamp B, Rümenapf T, Persson MA, Rey FA, Krey T (2012) High-level secretion of recombinant monomeric murine and human single-chain Fv antibodies from *Drosophila* S2 cells. Protein Eng Des Sel 25:59-66.

21. Melmed GY, Targan SR, Yasothan U, Hanicq D, Kirkpatrick P (2008) Certolizumab pegol. Nat Rev Drug Discov 7:641-642.

22. Lacey DL, Boyle WJ, Simonet WS, Kostenuik PJ, Dougall WC, Sullivan JK, San Martin J, Dansey R (2012) Bench to bedside: elucidation of the OPG-RANK-RANKL pathway and the development of denosumab. Nat Rev Drug Discov 11:401-419.

23. Wilkinson IC, Hall CJ, Veverka V, Shi JY, Muskett FW, Stephens PE, Taylor RJ, Henry AJ, Carr MD (2009) High resolution NMR-based model for the structure of a scFv-IL-1β complex: potential for NMR as a key tool in therapeutic antibody design and development. J Biol Chem 284:31928-31935.

24. Alexandrov AI, Mileni M, Chien EY, Hanson MA, Stevens RC (2008) Microscale fluorescent thermal stability assay for membrane proteins. Structure 16:351-359.

25. Otwinowski Z, Minor W (1997) Processing of X-ray diffraction data collected in oscillation mode. Methods Enzymol 276:307-326.

26. Kabsch W (2010) XDS. Acta Crystallogr D Biol Crystallogr 66:125-132.

27. McCoy AJ, Grosse-Kunstleve RW, Adams PD, Winn MD, Storoni LC, Read RJ (2007) Phaser crystallographic software. J Appl Cryst 40:658-674.

28. Emsley P, Lohkamp B, Scott WG, Cowtan K (2010) Features and development of Coot. Acta Crystallogr D Biol Crystallogr 66:481-501.

Table 1. Data collection statistics

	TNFα-certolizumab Fv complex	RANKL-denosumab Fv complex
X-ray source	BL41XU, SPring-8	BL41XU, SPring-8
Wavelength (Å)	1.0	1.0
Space group	$C2$	$I4_132$
Cell dimension		
a, b, c (Å)	101.4, 110.45, 133.6	192.5, 192.5, 192.5
α, β, γ (°)	90.0, 105.3, 90.0	90.0, 90.0, 90.0
Total No. of reflection measured	496486 (21314)	1128891 (80799)
No. of unique reflections	82561 (6027)	29117 (2123)
Resolution range (Å)	50-2.10 (2.15-2.10)	48.15-2.25 (2.31-2.25)
R_{merge}	11.0 (90.2)	20.6 (519.5)
Mean $I/\sigma(I)$	10.3 (1.97)	17.3 (1.40)
Completeness (%)	99.7 (98.8)	100.0 (100.0)
$CC_{1/2}$	99.6 (52.9)	99.9 (50.4)
Redundancy	6.0 (3.5)	38.8 (13.7)
V_M (Å^3 Da^{-1})	2.78	3.50
Solvent content (%)	55.8	64.9

Values in parentheses are for the outer shell.

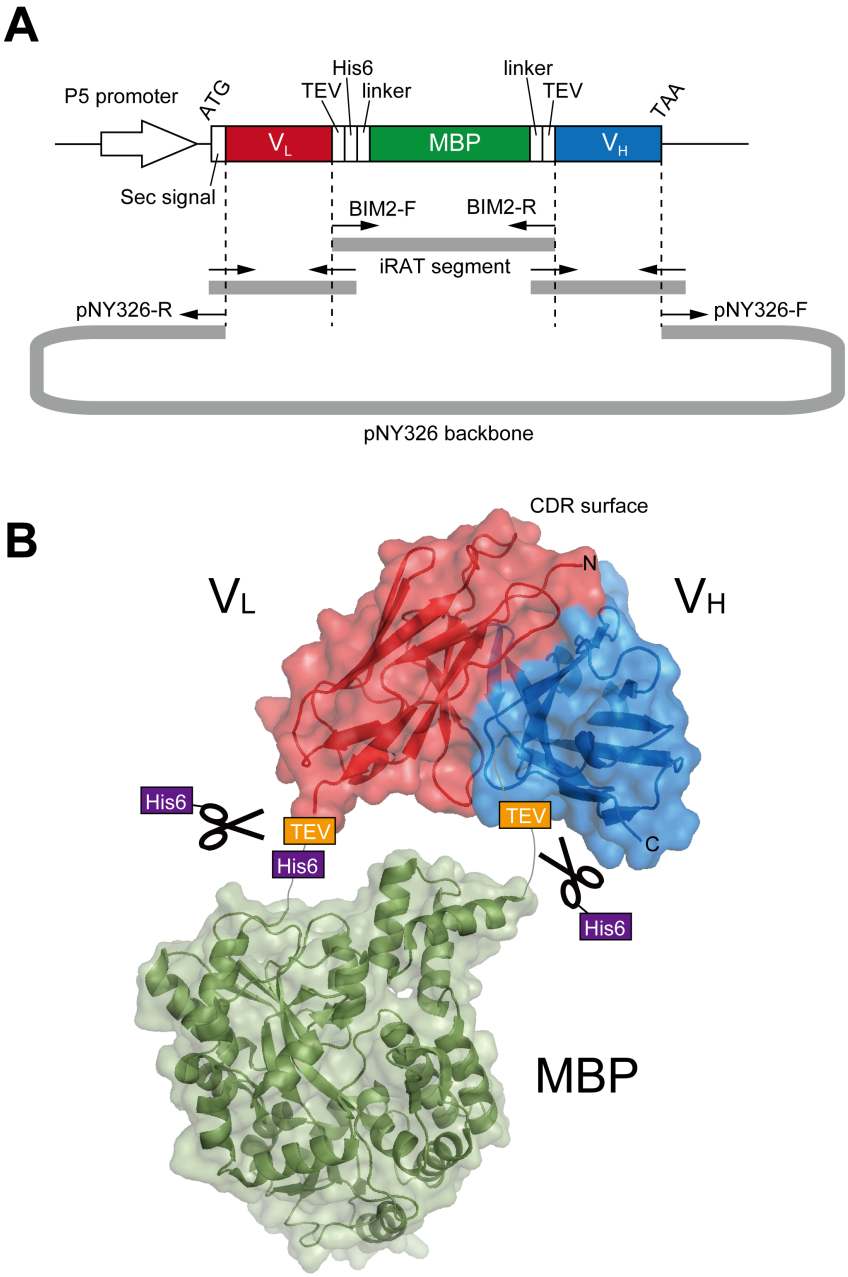

Figure 1. Expression construct for production of Fv fragments via iRAT system. (A) Schematic diagram and construction strategy of the pBIM2 plasmid. The V_L- and V_H-encoding cDNAs are amplified with PCR primers containing 27-nucleotides 5' overhangs, which act as 'guiding ends' in the subsequent Gibson assembly reaction. (B) iRAT-systhetic polyproteins are used to produce Fv fragments in high quality and quantity with *Brevibacillus* secretory expression system. The resulting polyproteins are recovered form the culture supernanant, purified by IMAC and excised with TEV-His_6 (indicated by 'scissors' icon). After removal of the iRAT portion and TEV-His_6 by reverse IMAC, non-tagged Fv fragments are further purified by SEC. V_L is colored in red, iRAT in green and V_H in blue. V_L N-terminus, V_H C-terminus and CDR surface are marked.

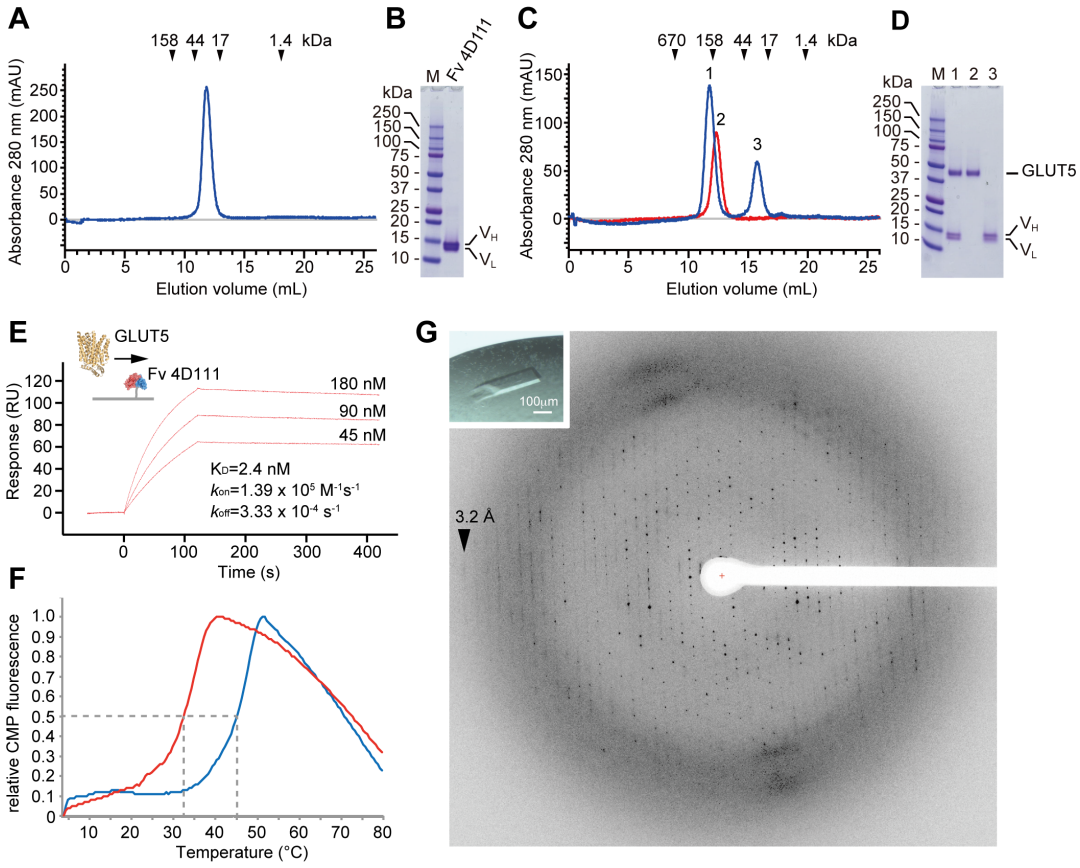

Figure 2. iRAT-based production and characterization of the Fv 4D111. (A) The concentrated final product from purification, analyzed by SEC on a Superdex75 10/300GL column. (B) SDS-PAGE analysis of the peak fraction of SEC in (A). (C) SEC profile for the isolation of GLUT5-Fv 4D111 complex in the presence of an excess of Fv 4D111 (blue line) on a Superdex200 10/300GL column. As a reference, GLUT5 alone was separated on the same column (red line). Elution volumes of protein standards are indicated at the top. Peak 1: GLUT5-Fv 4D111 complex, peak 2: free GLUT5, peak 3: free Fv 4D111. (D) SDS-PAGE analysis of the corresponding peak fractions in (C). (E) SPR sensorgrams for the association of GLUT5 (45, 90, 180 nM) with immobilized Fv 4D111 were fitted to 1:1 Langmuir binding model, giving the apparent dissociation constant (K_D), association rate constant (k_{on}) and dissociation rate constant (k_{off}) of complex formation. (F) Effect of Fv 4D111 on thermal stability of GLUT5 evaluated by CPM assay. GLUT5 alone was used as the control experiment (red line) compared to GLUT5-Fv 4D111 complex (blue line). (G) Representative X-ray diffraction of a crystal of the GLUT5-Fv 4D111 complex. An example of the complex crystals is shown in the inset.

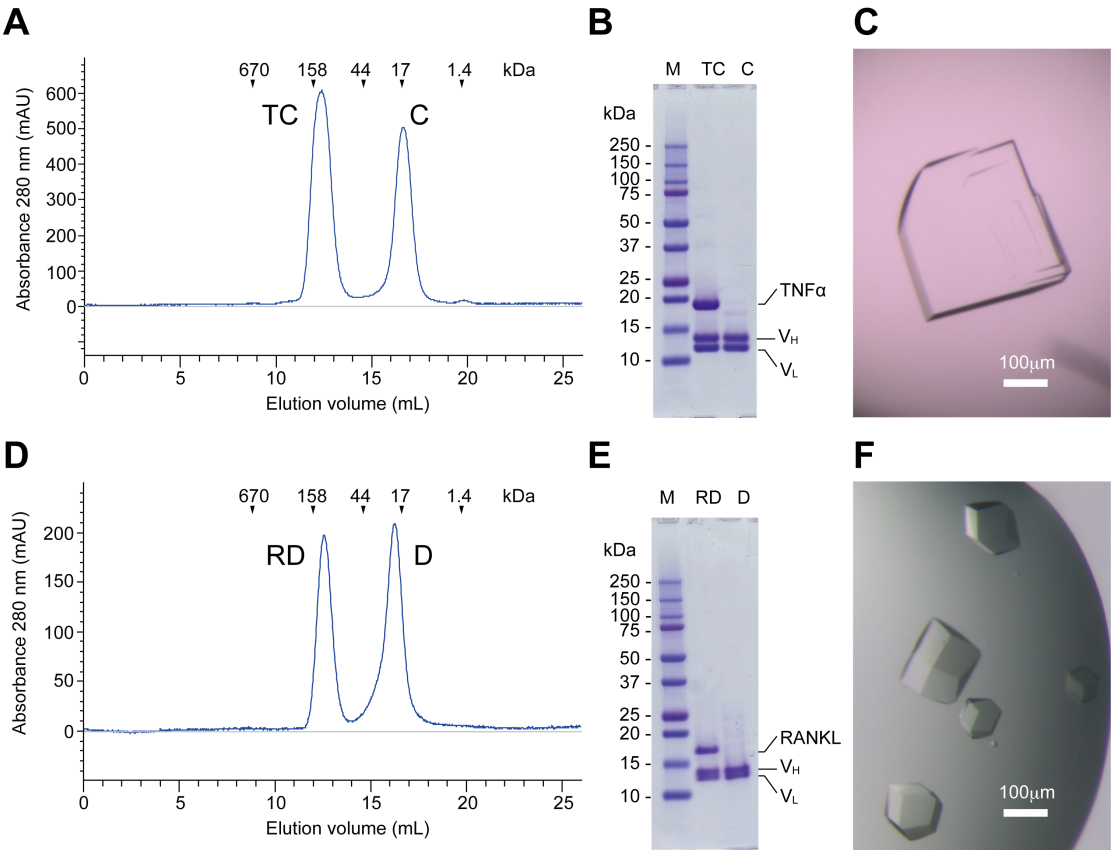

Figure 3. Fv fragments derived from the therapeutic antibodies, certolizumab and denosumab, produced via iRAT system. (A) A SEC chromatogram for the isolation of TNFα-certolizumab Fv complex in the presence of an excess of the Fv on a Superdex200 10/300GL column. Peak TC: TNFα-certolizumab Fv complex, peak C: free certolizumab Fv. (B) SDS-PAGE analysis of the corresponding peak fractions in (A). (C) Crystals of the TNFα-certolizumab Fv complex. (D) A SEC chromatogram for the isolation of RANKL-denosumab Fv complex in the presence of an excess of the Fv on a Superdex200 10/300GL column. Peak RD: RANKL-denosumab Fv complex, peak D: free denosumab Fv. (E) SDS-PAGE analysis of the corresponding peak fractions in (D). (F) Crystals of the RANKL-denosumab Fv complex.

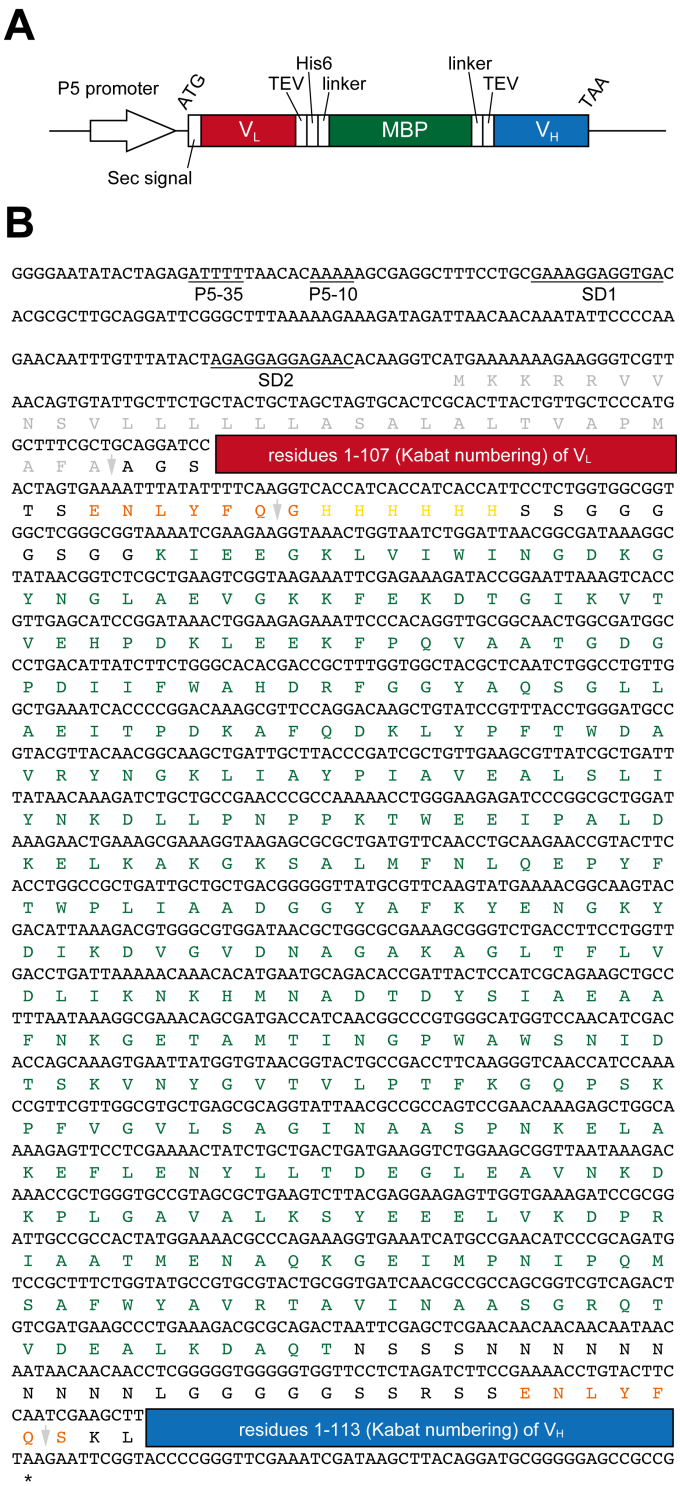

Supplementary Figure 1. Structure of the iRAT-based Fv expression vector pBIM2. (A) Schematic illustration of the region containing the promoter, secretion signal and iRAT-polyprotein construct. (B) Sequence corresponding to the region shown in (A). P5-35 and P5-10 represent the -35 and -10 box of the promoter P5, respectively. SD1 and SD2 are Shine-Dalgarno sequences. The Sec secretion signal, TEV recognition sequence, His_6 tag and MBP are shown in gray, orange, yellow and green, respectively. Gray arrowheads indicate the signal cleavage site and TEV cleavage sites.